Available online at www.sciencedirect.com

ScienceDirect

journal homepage: www.elsevier.com/locate/he

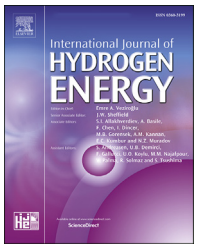

Experimental study of hydrogen production using electrolyte nanofluids with a simulated light source

Shihao Wei [a], Javad Hikmati [a], Boris V. Balakin [b,c], Pawel Kosinski [a,*]

[a] University of Bergen, Department of Physics and Technology, Bergen, Norway
[b] Western Norway University of Applied Sciences, Department of Mechanical and Marine Engineering, Bergen, Norway
[c] Department of Thermal Physics, National Research Nuclear University MEPhI, Russia

HIGHLIGHTS

- Successfully prepared a stabilized sodium sulfate electrolyte with carbon black nanoparticles.
- Hydrogen production increases with the increasing of the concentration of nanofluids then decrease.
- Carbon black nanoparticles have both positive and negative impacts on electrolysis.
- Using nanofluids can increase the efficiency of electrolysis.

ARTICLE INFO

Article history:
Received 21 June 2021
Received in revised form
2 December 2021
Accepted 13 December 2021
Available online 3 January 2022

Keywords:
Electrolysis
Carbon black
Nanofluids
Hydrogen production rate
Electrical properties

ABSTRACT

In this research, we conducted water electrolysis experiments of a carbon black (CB) based sodium sulfate electrolyte using a Hoffman voltameter. The main objective was to investigate hydrogen production in such systems, as well as analyse the electrical properties and thermal properties of nanofluids. A halogen lamp, mimicking solar energy, was used as a radiation source, and a group of comparative tests were also conducted with different irradiation areas. The results showed that by using CB and light, it was possible to increase the hydrogen production rate. The optimal CB concentration was 0.1 wt %. At this concentration, the hydrogen production rate increased by 30.37% after 20 min of electrolysis. Hence, we show that using CB in electrolytes irradiated by solar energy could save the electrical energy necessary for electrolysis processes.

Introduction

Because of the depletion of traditional energy reserves and their detrimental emissions into our ecosystem, hydrogen is recognized as the global future energy. So far hydrogen has been widely produced from hydrocarbon sources, initiating an enormous output of carbon dioxide and contaminants [1]. With renewable energy consumption on the rise as well as the global energy demand [2], electrolytic hydrogen production technologies offer a sustainable alternative to conventional hydrogen production methods [3]. Water electrolyser can utilize solar energy to generate hydrogen of high purity with

* *Corresponding author*. Universitetet i Bergen, Postboks 7803, N-5020 Bergen, Norway.
E-mail address: Pawel.Kosinski@uib.no (P. Kosinski).

https://doi.org/10.1016/j.ijhydene.2021.12.130

zero adverse emissions, at any location around the world with access to sunlight, due to its simplicity and flexibility [4].

The most important parameter of electrolysis is efficiency. A low efficiency can make the energy cost larger than the energy produced. There are many factors that can affect the efficiency of electrolysis. The most investigated, and also the most important, factor is the use of catalysts. Some researchers reported outstanding catalytic performance of chemical compounds at different electrolytes [5,6]. Furthermore, some nanocomposites can also be used as high-efficiency electrocatalysts in the water-splitting reaction [7–9]. Moreover, nanosized materials or nanostructures have good optical and electrochemical properties that can increase the thermal stability of electrolytes and electrolysis devices [10–15]. Finally, the excellent electrochemical performance also makes some nanocomposites be a potential hydrogen storage material [16].

It is also recognized that the main parameters influencing the heat transfer efficiencies of fluids are their thermal properties such as viscosity, density, heat capacity, and thermal conductivity, with the latter being the most influential factor [17]. Since base fluids (water, oil, and ethylene) possess low thermal conductivity, their solar absorption efficiency is also usually low [18]. Nevertheless, Maxwell [19] in 1873 proposed a mechanism that involves adding micro-sized particles into a base fluid to improve the heat absorption capability of the base fluid, and Choi and Tran [20] identified that adding even smaller particles to a base liquid could improve the heat transfer characteristics of the base fluid. They stated that the addition of nanoparticles (NPs) (solid particles with a diameter in the range of 1~100 nm) into conventional fluids raised thermal conductivity and defined these innovative classes of heat transfer fluids as nanofluids (NF) [21]. Compared to the absorption efficiency of water (13%) [22], carbon-based NF may absorb 96% of solar radiation [23].

Carbon black (CB) is one of several substances with analogous absorption characteristics as the ideal concept of a black body, which in theory absorbs all incident radiation [24]. Similarly, CB is a kind of material that has good absorption throughout the whole wavelength range of sunlight and has thus high potential for solar energy applications.

Sani et al. [25] experimented with carbon black nanoparticles (CB NPs) in distilled water (DW) and reported that the photothermal efficiency of CB was 85%. Another advantage of nanometre-sized particles is that they can pass through small passages, unlike micrometre-sized particles that cause severe clogging problems in heat transfer equipment [20]. Also, Han et al. [26] stated that 90% of incoming radiation can be absorbed by a thick layer of CB.

Multiple researchers agree that hydrogen production by electrolysis depends vastly on the temperature of the electrolyte. For instance, Galney et al. [27] designed a high-temperature alkaline electrolysis cell and tested it at a temperature between 35 °C and 400 °C. The electrolyte showed a significant performance enhancement at the higher temperature. Also, Brett et al. [28] investigated the enhancement in the hydrogen production rate via raising the temperature of the electrolyte. The accumulated heat of the sun through a heat absorber material can thus be coupled with electrical energy in a conventional water electrolyser to improve production efficiency.

Electrolyzing NF-based electrolytes is a new research field. Some investigation has been carried out to describe the electrical properties of NFs according to different NPs, size, volume fraction, etc. Lobato et al. [29] discovered that nanofluids with a 0.04 wt% of carbon nanoparticles attained higher charge capacities and energy efficiencies at higher current densities. Bose et al. [30] reported that the ionanofluid (ionic liquid-based nanofluid) electrolyte delivered a higher discharge capacity than a conventional electrolyte. Moreover, Yen et al. [31] utilized the dimensional analysis method to investigate the Al_2O_3 water-based nanofluid. The results showed the Al_2O_3 nanofluid with the emulsifying agent had the highest electric charge density at 40 °C and 2.5 wt%.

The studies mentioned above were focused on the thermal or electrical properties of nanofluid-based electrolytes. At present, there is no report in the literature concerning both properties. Similarly, no study focuses on the hydrogen production of electrolyzing nanofluid-based electrolytes. Therefore, the main purpose of this work is to investigate these issues.

Experimental method

Nanofluid preparation

The experimental procedure of nanofluid preparation is shown in Fig. 1. Firstly, the suitable weight fractions of CB nanoparticles (Ensaco 350G Carbon Black, Timcal) and surfactants (sodium dodecyl sulfate, SDS) were weighed and blended with distilled water. Each component was using a Sartorius CPA 324 S balance. To acquire a more uniform mixture, the suspension was stirred for 5 min using a ceramic magnet stirrer plate with a magnetic stirrer bar. Meanwhile, the tank of a Branson 3510 ultrasonic cleaner (a bath sonicator) was filled with tap water to the operating level line (3 cm from the top) and degassed for 10 min to eliminate bubbles formed in the water. The cleaner had a frequency of 40 kHz and a maximum power of 335 V with a maximum capacity equal to 6 L. Secondly, the stopwatch was set to 60 min before

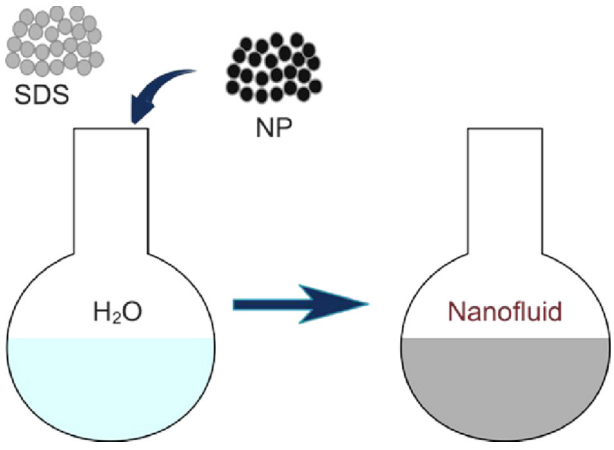

Fig. 1 – Two steps of NF preparation.

carefully locating the beaker containing the solution within the tank. As waves are transferred and distributed throughout the water, the beaker must therefore not touch the tank bottom (beaker floats). The beaker was submerged in the water bath, and the level of the water tank was higher than the level of the solution inside the beaker.

Several authors emphasize the duration of sonication as a crucial step for NF preparation. Asadi et al. [32] investigated the impact of sonication time on various NPs and emphasized that for most NPs the optimum sonication time was between 20 to 40 min. For comparison, samples with a varied sonication time of 10, 20, 30 and 60 min were prepared in this work. The samples that were sonicated for 20 min showed greater improved stability than those that were sonicated for 10 min. When the concentration of NF was larger than 0.1 wt%, 30 min of sonication was not sufficient to acquire a stable NF. Therefore, all the samples were sonicated for 60 min in this work, as mentioned previously.

Following the chemical and physical treatments of NFs, a sodium sulfate (SS) electrolyte was subsequently added and stirred for a minimum of 5 min with a magnet stirrer before discharging the electrolyte solution from the upper opening of the electrolysis apparatus into the bubble-shaped reservoir of a Hofmann voltameter (see Fig. 2). The anode and cathode compartments were filled by stirring the valves at the upper end of the two cylindrical tubes. Given that the adsorption of SDS decreases with temperature, one drop of Antifoam B Emulsion was added to the solution to minimize the risk of foam formation.

SS is a neutral salt, so the pH of its aqueous solution is around 7. As it has been tested by many researchers, pH has a significant impact on the stability of nanofluids. When pH value is below 7, nanofluids show a significant enhancement on stability with the increasing of pH value until 7. However, when pH is above 7, sedimentation occurs [33]. Therefore, we chose SS solution as the electrolyte as it has less impact on the stability of nanofluids.

In this study, nanofluids with different weight percent concentrations (0.005 wt %~1 wt %) were manufactured. Hwang et al. [34] suggest that using 1 wt % SDS improves the stability of carbon-based nanofluids. Therefore, the same amount of this surfactant was added to all the samples.

Surfactant is an important compound to stabilize the colloid because surfactants can attach to the particle surfaces to form micelles. This hinders the agglomeration of the dispersed phase. According to our study, SDS has excellent performance on stabilizing CB-based nanofluid [35,36]. On the other hand, SDS can be harmful to the environment as it can produce sulfates and persulfates at high concentrations [37]. Therefore, many researchers have started to study the environmental impact and biodegradability of the mixture of surfactants and nanoparticles. Here, alkyl polyglucoside, a non-ionic surfactant, has been considered [38]. Therefore, we are planning to investigate the feasibility to use this surfactant to prepare CB nanofluid in our future work.

Experimental procedure

Hydrogen production was investigated by using a Hoffman voltameter, where the volume of hydrogen produced by

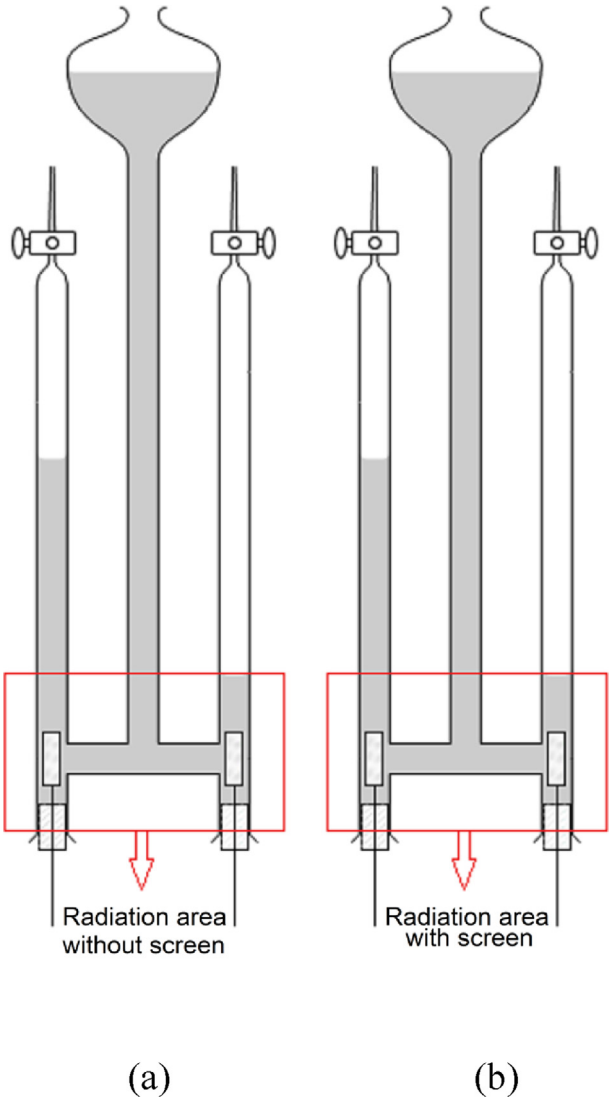

Fig. 2 – The scheme of Hoffmann voltameter irradiated by the artificial light: (a) without the protective screen/collimator; (b) with a protective screen/collimator (irradiation occurs only in the marked area).

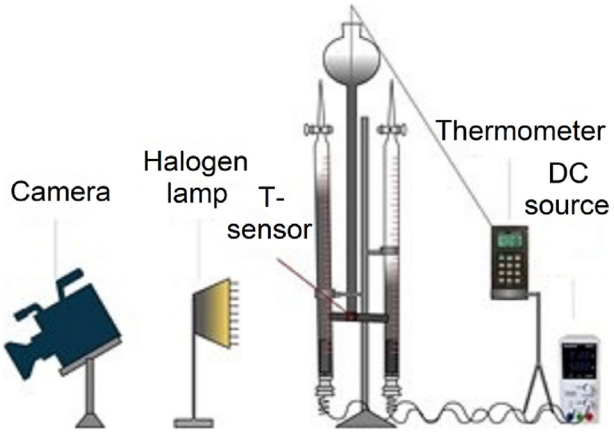

Fig. 3 – Schematic representation of experimental apparatus.

electrolysis can be read directly from the scale on the pipe. Fig. 3 shows the framework of nanofluid-based electrolysis experiments. The DC source from Peakteck, and its maximum output current and voltage, are 2 A and 30 V with the measurement accuracy within ±1% + 5 digits, respectively. The temperature was measured by thermocouples and recorded through an Omega HH506RA thermometer with an error range of ±0.05%. A Cotech 400 W/230 V flood-light halogen lamp with an Osram 400 W/230 V R7S light bulb was used to simulate the solar irradiation. The meter from Linshang Technology with an accuracy of ±0.10% measured the irradiance intensity. After preparing the nanofluids as described in Section Nanofluid preparation, we let the nanofluids stay still to cool down. The 1-h sonification made the temperature of the nanofluid higher than the room temperature. When the temperature of the nanofluid reached 30 °C, the camera, the lamp and the DC source were simultaneously turned on. The lamp directly illuminated the area near the electrodes, which is denoted as the rectangle in Fig. 2. The temperature, electric current and hydrogen volume were recorded every 2 min.

The reactions for SS in this work were as follows:

$$\text{Anode: } 4OH^- - 4e^- = 2H_2O + O_2 \quad (1)$$

$$\text{Cathode: } 4H^+ + 4e^- = 2H_2 \quad (2)$$

$$\text{Overall Reaction: } 2H_2O = 2H_2 + O_2 \quad (3)$$

In this work, we focused on three issues influencing hydrogen production. First, to investigate the electrolyte effect on hydrogen production, the electrolysis was performed at ambient temperature in the range of 20~26 °C. All tests excluding NF and light are conducted in the darkroom for a particular amount of time with SS concentration in the range of 1~12 wt%, while keeping a constant applied voltage (30 V). The darkroom means there were only natural light sources in the room, and the light intensity was below 100 W/m^2.

Subsequently, the experiments were performed under the presence of the halogen lamp, while holding other parameters constant (voltage and SS wt.%). The centre of the halogen lamp and the electrolytic plates were fixed on the same level to ensure the core zone of electrolysis could be illuminated by the maximum radiation, see Fig. 2 (a). The radiated heat flux coming from the halogen lamp resulted in the temperature increase of the electrolyte. The elevated temperature gave rise to a higher current density in the electrolyser. The highest current density for the maximum voltage and electrolyte concentration was 0.3 A/cm ^{2}.

Afterwards, the experiments were conducted with CB coupled with the halogen lamp. The effect of CB on hydrogen production was studied as follows: (i) the effect of light intensity was investigated by changing the distance between the electrolyser and the radiation source, thus influencing the irradiance intensity, while keeping the other parameters constant; (ii) the experiments were performed with CB concentrations in the range of (0.005–1.0) wt.%, while SS concentration and the distance to the radiation source were kept constant. Considering that some metal elements (the wires and electrodes) could absorb heat, which has a negative impact on experimental results, i.e., those mental elements could absorb heat and cause the temperature to increase faster, a set of comparative tests was conducted. For comparative tests, a 5 mm thick screen with a small hole (20 mm × 30 mm) was set between the halogen lamp and Hoffman voltameter. The radiation area is shown in Fig. 2 (b), where the red rectangle has the same size as the small hole in the screen. Therefore, only this area was irradiated by the light. It could ensure that the core zone of electrolysis was illuminated by the light, but it also eliminated the heat absorption by the metal elements.

Results and discussion

Experimental results for single variables

The effect of CB-based nanofluids on water electrolysis has not been done in the research literature yet. Therefore, many factors may affect experimental results. Generally, the optical properties of nanofluids are one of them. Thus, experimental results of water electrolysis using salt electrolyte and CB nanofluids conducted in dark and light environments are presented in this section.

(1) *The dark and light environments*

Fig. 4 shows the results of electrolyzing the SS solution with different concentrations. These experiments were conducted in the dark environment and light environment, respectively. The irradiance of light was 1000 W/m^2 (i.e., 1 sun), and the processing time was 20 min. We observed a similar linear trend that the hydrogen production rate increased with the increase of SS concentration for both dark and light environments. According to the results, the rate of hydrogen production for the environment with light (1.88 ml/min) was higher than for the dark room (1.5 ml/min), as

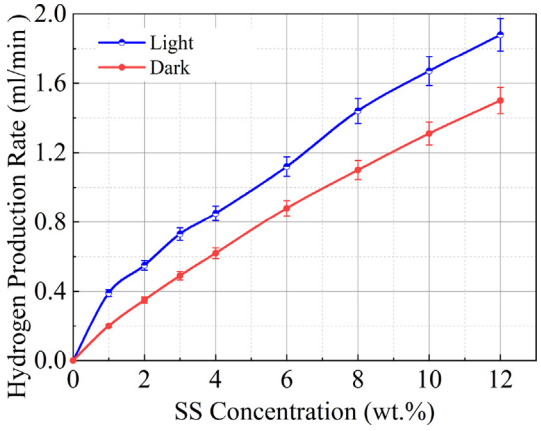

Fig. 4 – Hydrogen production rate for light and dark environments, for different SS concentrations.

expected. This occurred for SS concentration equal to 12 wt%. Thus, the light radiated the nanofluid and increased the temperature. The higher temperature accelerated the movement of ions in the electrolyte that facilitates the dissociation of water. As a consequence, a higher temperature decreases the voltage needed for electrolysis, i.e., the consumption of electricity.

This can also be explained by analysing the fundamental relation for Gibbs energy of water electrolysis in standard conditions [39]:

$$\Delta G_d^{\circ}(H_2O(l)) = \Delta H_d^{\circ}(H_2O(l)) - T\cdot\Delta S_d^{\circ}(H_2O(l)) \tag{4}$$

where ΔG is Gibbs energy, ΔH is enthalpy and ΔS is entropy.

The process of a water splitting reaction requires energy input, and this energy is almost constant within the experimental environment. That means the variation of ΔH with temperature can be omitted. For electrolysis, the Gibbs energy is the required electrical energy. Therefore, from Eq. (4), when ΔH remains constant, increasing T means decreasing ΔG. Thus, Gibbs energy decreases with the increase of the operating temperature.

(2) *Carbon black*

In our next experiments, 0.05 wt% of CB was added to the electrolyte. The reaction time was again 20 min. All the samples were added SDS, and the concentration of SS was the only variable in the experiments. It must be noted that SDS could not only stabilize the nanofluids, it also increased the electrical conductivity of the electrolyte [40,41]. The results of the experiments are collected in Fig. 5.

Adding CB into an SS solution can increase the hydrogen production rate, as mentioned previously, because NPs could increase the electrical conductivity of the electrolyte. Some researchers indicated that carbon-based nanoparticles could increase the conductivity of the solutions, and the maximum values were obtained for the concentrations about 0.2 wt% [42,43]. In electrolytes, electrical conduction occurred by motion of ions. Therefore, higher electrical conductivity means the faster movement of ions can facilitate electrolysis. Maxwell [44] showed a model that was considered applicable, mostly for estimating the electrical conductivity of a nanofluid. This model is a function of the electrical conductivity of nanoparticles and the base fluid:

$$\frac{\sigma_{nf}}{\sigma_{bf}} = 1 + \frac{3\left(\frac{\sigma_p}{\sigma_{bf}} - 1\right)\varphi}{\frac{\sigma_p}{\sigma_{bf}} + 2 - \left(\frac{\sigma_p}{\sigma_{bf}} - 1\right)\varphi}, \tag{5}$$

where σ_{nf} is the electrical conductivity of the nanofluid; σ_{bf} is the electrical conductivity of the base fluid; σ_p is the electrical conductivity of the particles and φ is the concentration of the solution.

In our experiments, Brownian motion and electrophoretic mobility are also vital factors that could affect the electrical conductivity of the nanofluid. Shen et al. [45] combined these two factors and the updated Maxwell model. The model for electrophoretic mobility can be written:

$$\sigma_E = \frac{2\varphi\varepsilon_r^2\varepsilon_0^2 U_0^2}{\eta r^2}, \tag{6}$$

where σ_E is the electrical conductivity due to electrophoretic mobility; ε_r is the dielectric constant of base fluid; ε_0 is the dielectric constant of vacuum; U_0 is the zeta potential of nanoparticles; η is the viscosity of the nanofluid and r is the radius of nanoparticles.

Also, the model for Brownian motion is as follows:

$$\sigma_B = \frac{3\varphi\varepsilon_r\varepsilon_0 U_0\left(\frac{RT}{L}\cdot\frac{1}{3\pi\eta}\right)}{r^{\frac{3}{2}}} \tag{7}$$

where σ_B is the electrical conductivity caused by Brownian motion, R is the thermodynamic constant, T is temperature and L is the Avogadro constant.

Therefore, the total electrical conductivity for nanofluid becomes:

$$\sigma = \sigma_{nf} + \sigma_E + \sigma_B. \tag{8}$$

(3) *Light and carbon black*

Fig. 6 and Fig. 7 show histories of hydrogen volume and temperature during the experiments. The curves represent

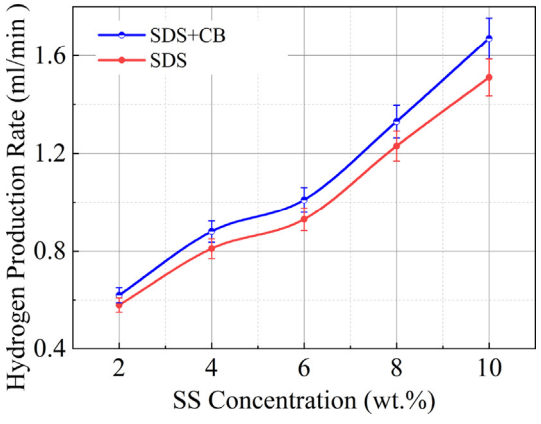

Fig. 5 – Hydrogen production rate for different SS concentration.

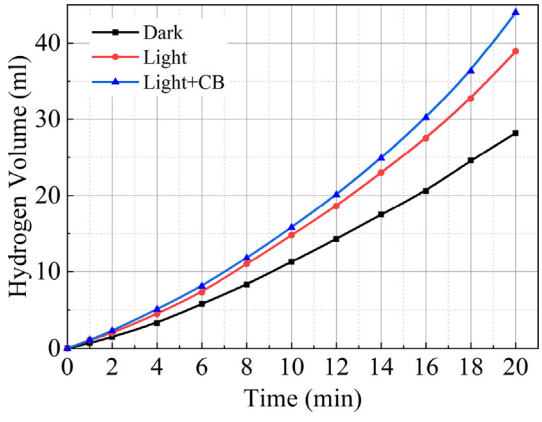

Fig. 6 – Hydrogen volume variation with time for tests in different environments.

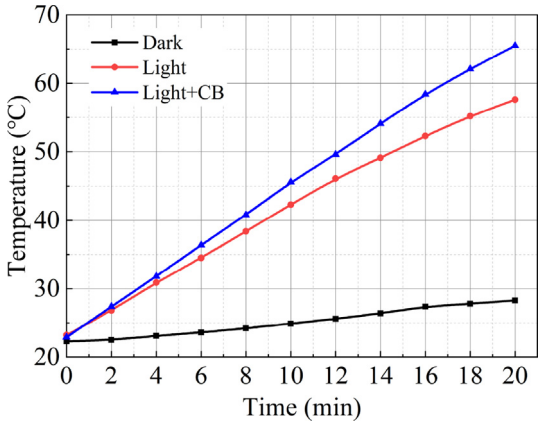

Fig. 7 – Temperature variation with the time in different environments.

the results of the experiments carried out for three cases: (i) in a dark environment, (ii) with light, and (iii) for CB based solutions. The intensity of light was 1000 W/m^2, and the concentration of CB and SS was 0.05 wt% and 10 wt%, respectively. SDS was added to all the electrolytes. The general conclusion from the results is that using a nanofluid-based electrolyte has a positive impact on electrolysis as an increased temperature can speed up the reaction rate. From Figs. 6 and 7, the temperatures after 20 min were 65.5 °C, 57.6 °C and 28.3 °C, from the top to the bottom. The maximum temperature (Fig. 7) increased 103.53% and 131.45% for the case with only light, and light with CB, respectively.

Lavasani et al. [46] used graphene-based nanofluids to investigate the thermal conductivity enhancement for different weight fractions, and their results showed that the increase in thermal conductivity at high temperatures becomes more prominent by increasing weight percentage. The increase of the fluid temperature is also associated with the increase in hydrogen production. The maximum volume of hydrogen increased by 37.94% and 56.03% for light and light and CB, respectively (Fig. 6). It is easy to see the direct effect of temperature on hydrogen production from Fig. 7. Although both electrical conductivity and temperature could increase the hydrogen production, when comparing the three initial conditions, the temperature had a more obvious effect on it. In addition, the electrical conductivity increases with temperature due to the enhanced Brownian motion, see Eq. (7).

Heyhat et al. [47] found that the electrical conductivity of carbon-based nanofluids increased with the increase of temperature and nanofluid concentration. The maximum augmentation was for temperature 25 °C and the minimum occurred in the temperature 55 °C. Also, the effect of increasing the nanofluid concentration was stronger than temperature. This observation does not directly correspond to our experimental results. Comparing Figs. 4 and 5, the temperature effect (using light) is more significant than that of CB concentration because the hydrogen production rates increased more.

In our research, the impact of different irradiance of light was also studied for the electrolyte with CB and without CB. The values of irradiance were 1000 W/m^2, 1500 W/m^2 and 2000 W/m^2 and are denoted respectively as black, red, and blue lines in Fig. 8. The results showed the higher irradiance induced higher temperature, and CB intensified the process. It is worth noting that the temperature can still be rather high even without CB. The maximum temperatures in Fig. 8 (a) were 67.3 °C, 61.7 °C and 57.6 °C. Also, according to Fig. 7 (b), the values were 82 °C, 70.7 °C and 65.5 °C. Thus, the presence of CB increased the temperature by a factor of 21.84%, 14.59% and 13.72%, respectively.

Effect of CB concentration

In Section Experimental results for single variables, the optical properties of electrolyte were investigated. In this section, however, we focus on the photothermal properties and electrical properties as they have a vital role in the process of energy transformation. The objective of this part of the study is to investigate how the concentration of CB affects the hydrogen production rate. To minimize the influence of temperature on the results, the ideal gas law was used to modify the hydrogen volume measured during the experiments. The modified hydrogen volume is the volume of hydrogen at room temperature, i.e., we eliminate the volume expansion of hydrogen volume at high temperatures. This can be calculated from the following:

$$V_1 = V_0 \frac{T_1}{T_0} \tag{9}$$

where V_1 is the modified hydrogen volume; V_0 is the hydrogen volume measured in the experiments; T_1 is the room temperature and T_0 is the temperature measured in the experiments.

The findings from the previous sections revealed an improvement in hydrogen production rate, which was attributed to the higher temperature stimulated by the CB NPs. To examine the consequence of NF density, viscosity, and the applicability of higher NF concentrations for hydrogen production, several experiments were accomplished with CB concentrations in the range of 0.005~1 wt% together with comparative experiments. Each experiment was performed using constant SS concentration (10 wt%), constant radiation intensity (1000 W/m^2), and the same reaction time (20 min).

The maximum hydrogen volume that was calculated as the volume at room temperature for each experiment and conducted without the screen is depicted by a red line in Fig. 9. The modified generated hydrogen volumes (i.e., calculated from Eq. (9)) with the increase of CB weight percentage were 26.56 ml, 29.59 ml, 31.65 ml, 32.55 ml, 34.33 ml, 34.96 ml, 36.13 ml, 33.13 ml, 33.03 ml, 32.68 ml, 32.18 ml, 30.52 ml, respectively. As seen, the highest hydrogen volume obtained was 36.1 ml with a CB concentration of 0.1 wt%, whereas the lowest hydrogen volume (26.56 ml) resulted from the lowest CB concentration (0.005 wt%). According to Fig. 9, hydrogen production increased first and then decreased with the rising of the CB concentration. When the CB concentration was lower than 0.1 wt%, the hydrogen production increased rapidly with concentration. However, for higher concentrations, the influence of the concentration was less significant. The experimental results illustrate that the optimum hydrogen volume was produced for lower CB concentrations.

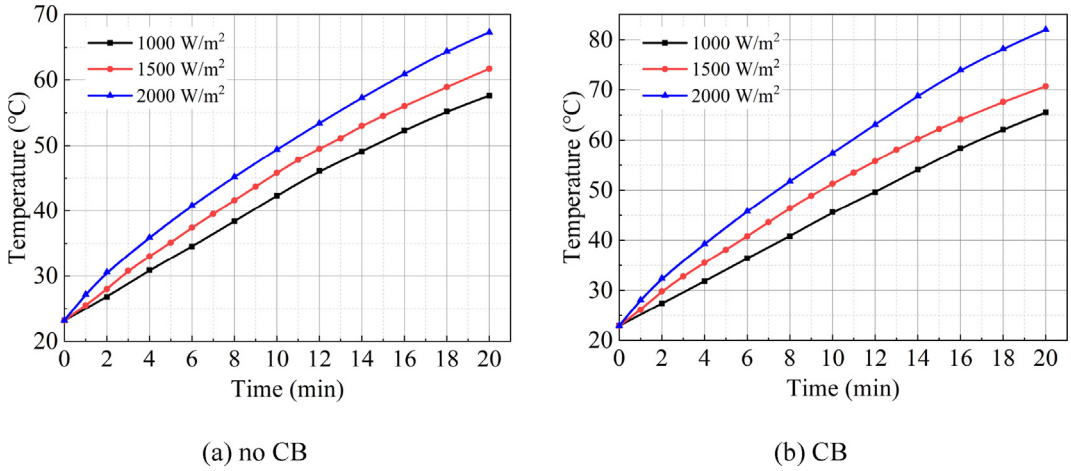

Fig. 8 – Temperature vs. time for different values of light irradiance: (a) no CB was used in the electrolyte; (b) the electrolyte contained 0.05 wt.% CB.

As the fraction of CB particles exceeds 0.1 wt%, the hydrogen volume declines. This is due to the fact that, apart from the influence of temperature, electrical conductivity increases with the rising of nanoparticle concentration as it strengthens Brownian motion and electrophoresis, see Eqs. (6) and (7) [48]. Zawrah et al. [49] also demonstrated this behaviour and noticed a following decrease of electrical conductivity when concentration increases. They explained this phenomenon as the complex processes related to the electrical double layer (EDL). The interaction between the nanoparticles and the EDL is the reason for the augmentation of electrical conductivity. However, with the increasing of the particle numbers, the charges available for the formation of EDL are insufficient and the electrostatic attraction force becomes a repulsion force among nanoparticles [49].

In addition to electrical conductivity, temperature is also a vital factor that affects the hydrogen production rate. An increase in particle concentration should increase the temperature of the nanofluid because more particles absorb heat. However, when the concentration reaches a certain range, nanoparticles form a "shield" in the outer nanofluids that blocks light from penetrating the nanofluids. In other words, for high particle concentrations, radiation cannot penetrate the system so that the heat transfer is dominated by conduction and convection. In addition, the rising of concentration induces higher viscosity [43], which hinders convection in the nanofluids. As a result, the heating process in the bulk of the fluid decreases.

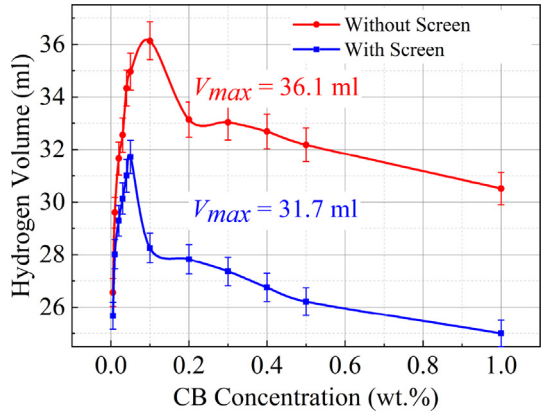

Fig. 9 – Hydrogen production vs. different CB concentration.

The blue line in Fig. 9 shows the results when the screen was used. The modified generated hydrogen volume with the increase of CB weight percent was 25.67 ml, 28.01 ml, 29.29 ml, 30.13 ml, 31 ml, 31.72 ml, 28.25 ml, 27.82 ml, 27.36 ml, 26.75 ml, 26.21 ml, 25 ml, respectively. This curve has the same trend as the red line, but the values are significantly lower. Moreover, it is worth noting that the maximum volume of hydrogen production occurred for concentration 0.05 wt %. In these experiments, only a small part of the nanofluids was illuminated by light. Under the same heat flux on the front face of a Hoffman voltameter, the radiation area was smaller than the experiments without the screen. As a result, the total energy that could be absorbed was also smaller. Although the radiation area was smaller here, the heat dissipation area was the same, i.e., the part of the Hoffman voltameter filled by the electrolyte. Thus, lower energy and nearly the same heat loss led to lower temperature increasing, and then less hydrogen production. When the temperature increased, the heat loss still increased so that a maximum total temperature occurred. This could be the potential reason that induces the maximum value for the concentration of 0.05%.

Fig. 10 (a) shows the modified hydrogen production rate for every 2 min for different CB concentrations. Five selected concentrations (0.02 wt %, 0.04 wt %, 0.05 wt %, 0.1 wt %, 0.2 wt %) are depicted in the figures. During the first 4~6 min, the hydrogen production rate was similar for all the studied concentrations. After 6 min, the rates still kept a rising tendency on average, but it was rather low except for a concentration of 0.1 wt %. During this time, all the rate curves show oscillations, and the amplitudes for the concentrations greater than 0.1% are higher than for the lowest concentrations. After 16 min, the hydrogen production rate showed a rising trend again. It also easily seen from Fig. 10 (a) that the average rates for different concentrations have a significant

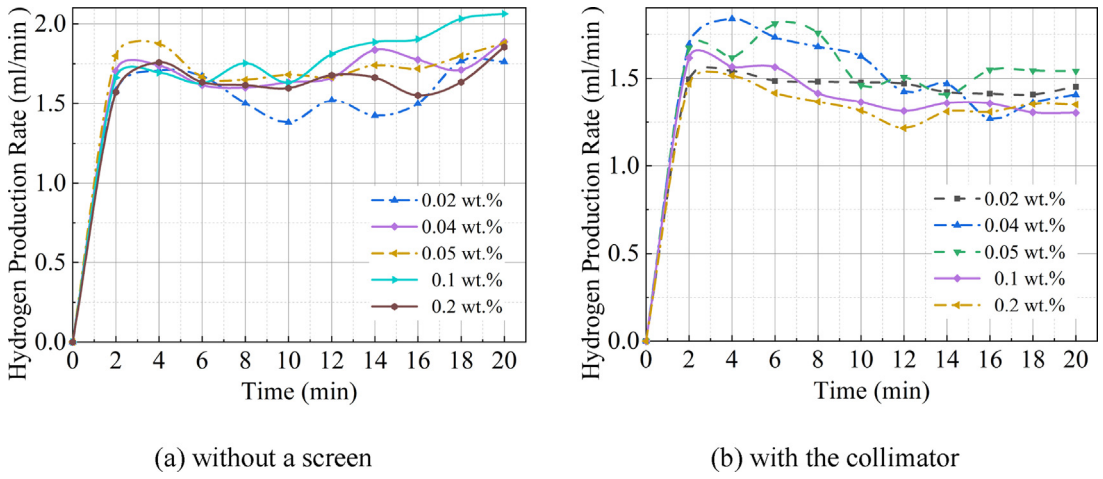

Fig. 10 – Hydrogen production rate variation vs. time for different CB concentrations: (a) no protective screen was used; (b) the voltameter was irradiatied by using a protective screen/collimator.

difference. The rates increased first and then decreased with the rising concentration, and the maximum showed a 0.1 wt %. A suitable concentration of nanofluids can increase the conductivity of the electrolyte, but too high concentrations of nanofluids might hinder the movement of electrons and decrease the hydrogen production rate. The hydrogen production rates during the whole processes of electrolysis can be treated as unstable oscillatory rising processes. Apart from the aforementioned effects of the heat transfer process and the variation of electrical conductivity, there are some possible explanations for this phenomenon.

On the one hand, the concentration of nanofluids increased as the electrolysis progressed because the water was electrolyzed. Similarly, the concentration of sodium sulfate solution also increased. Both have critical concentrations that led to some optimal hydrogen production, and a higher concentration of nanoparticles results in agglomerations and coat formations at the anodes, which has deteriorating effects on electrolysis [50]. Furthermore, the temperature kept increasing during the whole process, which could facilitate the electrolysis. This is discussed in the next section. Two different phenomena induced the oscillation in the curves. When the concentration was greater than 0.1 wt %, the nanofluids were more prone to be unstable and non-uniform and more disorder in the electrolyte induced greater oscillation amplitudes. From Figs. 4–6 temperature has a stronger effect on the electrolysis, which is reflected in the production of more hydrogen. Therefore, combining with the results in Fig. 10 (a), the whole trend should be increasing.

Fig. 10 (b) shows the results of the experiments with the collimator. The difference from the experiments without the screen is that the whole trend for these curves is falling. As stated before, the smaller energy source did not allow the system to reach the optimal temperature for the reaction, which means it is difficult to allow the positive to impact greater than the negative. Almost all the positive impacts are related to the temperature, including the reaction rate, electrical conductivity and some thermal properties of the electrolyte. They will change in a positive direction with the temperature rising. However, all the negative impacts are connected to the concentrations, like CB concentration, SS concentration, etc. Given that the essence of electrolyzing the SS solution was electrolyzing water, the concentrations can only increase. In other words, negative impacts will augment with time. In that case, negative impacts are much easier to show at lower temperatures than higher temperatures with the rising of concentrations. In this study, only the small radiation area could absorb heat, see Fig. 2 (b), and this part transfers the heat to the rest of the system. Furthermore, the two vertical pipes of the Hoffman voltameter had a larger surface area than the horizontal pipe within the radiation area, which means the high-temperature zone had a small dissipation area (the horizontal pipe) and the cold zone had a greater dissipation area (the two vertical pipes). This results in a large temperature gradient in the system, and the higher the temperature in the irradiated zone, the greater the gradient. On one hand, the temperature gradient could destabilize the nanofluid, and make nanoparticles easier to aggregate. The heat flow invokes convective currents in the system that could push the nanoparticles to move from the high temperature zone to the low-temperature zone. This increases the probability of contact and collision. More specifically, there were more particles near the electrodes than the area near the screen. In a colloidal system, charged ions adsorbed onto the surface of particles. As a result, the increasing number of nanoparticles in some areas made the charges available for the formation of an electrical double layer insufficient [49]. The electrostatic attraction becomes more than a repulsion force that destroys the stability of nanofluids. On the other hand, the temperature gradient could inhibit the electrolysis, and the larger the gradient, the stronger the inhibition. The mass flow caused by a temperature gradient, as well as electrophoresis, led charges to move to the electrodes (followed by the nanoparticles), which was inconsistent with electrolysis. Hence, this imbalance of potential in the electrolyte affected the progress of the water splitting reaction. Therefore, these two reasons may have caused the whole production rate to develop a falling trend.

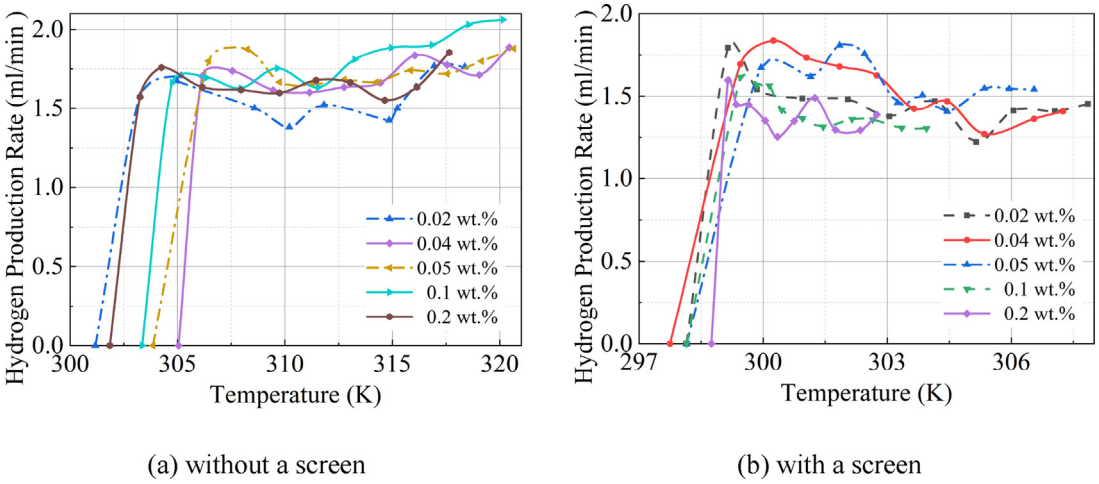

Fig. 11 – Hydrogen production rate for different CB concentrations vs. temperature: (a) no protective screen was used; (b) the voltameter was irradiatied by using a protective screen/collimator.

Effect of temperature

According to the discussion in Section Effect of CB concentration, the temperature plays an important role during the process. It was shown that the presence of CB nanoparticles increases the fluid temperature. In this section, however, we focus on how the temperature increase affects electrolysis and hydrogen production. Fig. 11 (a) shows the relationship between the modified hydrogen production rate and temperature without a screen. The graph makes it easier to conclude that the hydrogen production rate increased as the temperature increased. Also, the graphs in Fig. 11 (a) clearly show three stages: hydrogen production rate rapid rise stage, steady stage, slow rise stage. In the first stage, the hydrogen production rate increased very fast and reached the first extreme value (about 1.7 ml/min), while the temperature was below 305 K. When the temperature reached 305 K, the increase of hydrogen production rate seems to be paused until the temperature was greater than 315 K. In the third stage, the temperature increased again. However, the increase rate at this stage was less than the rate at the first stage. The maximum temperature occurred when the concentration was 0.1 wt %.

As we mentioned before, the higher CB concentration can increase the heat absorption ability of the electrolyte, and it can cause the temperature of the electrolyte to increase quickly when illuminated by light. Similarly, a higher temperature can increase the electrolytic velocity, thus causing an increase in the hydrogen production rate. However, a higher CB concentration does not mean a greater rate of hydrogen production. Compared with Figs. 10 (a) and 11 (a) also shows oscillations for rate curves with the increasing of temperature but does not show any linear trend as expected. This proves these two side effects exist and connect with temperature and CB concentration. There is a possible reason that can explain this phenomenon. Firstly, even though nanoparticles can increase the conductivity of the electrolyte, there are inhibitory effects that have negative impacts on electrolysis. For example, every single CB particle is charged due to the electrical double layer. With the increase of the temperature, mass flow and convection become stronger. Considering Brownian motion and electrophoresis, the movement of particles is highly random, which causes the uneven distribution and irregular movement of charges. On the other hand, the CB concentration increases as the reaction progresses. Thus, the electrical conductivity decreases when beyond the critical concentration. Moreover, in this study, SS functioned as a kind of salt that destabilized the nanofluid at higher temperature, which could also affect electrolysis. These negative effects together with positive effects (increasing electrical conductivity and reaction rate) caused the oscillations. Therefore, at the first stage, the electrolysis proceeded normally. When reaching the second stage, negative effect became prominent, so the rate increase paused. Nonetheless, at the third stage, since the temperature was high enough, the rate restarted and increased accordingly.

Fig. 11 (b) reveals how temperature affects the hydrogen production rate when using a screen. The whole curves can be divided into two parts as they have a similar trend as in Fig. 11 (a): a rapid rise stage and steady stage. At first, the rates increase faster and then decrease until 304 K. When the temperature is greater than 304 K, all the curves maintain dynamic stability. There are two differences compared with Fig. 11 (a): decreasing and no second increasing. The aforementioned statement could also be used to explain this. The temperature gradient strengthened the negative effects so that these two side effects could not maintain a balance at a relatively low temperature. Likewise, from Fig. 11 (b), the hydrogen production rates stayed within a certain range when the temperature reached 304 K and did not increase at a higher temperature. This phenomenon just proved that the temperature must reach a certain value to make positive effects stronger than negative effects. In these experiments, the critical temperature is 315 K. It should be emphasized that the larger heat loss and CB agglomeration could also affect the results.

That the temperature increases with an increasing of CB concentration, and then decreases, as shown in Fig. 11 (a), was

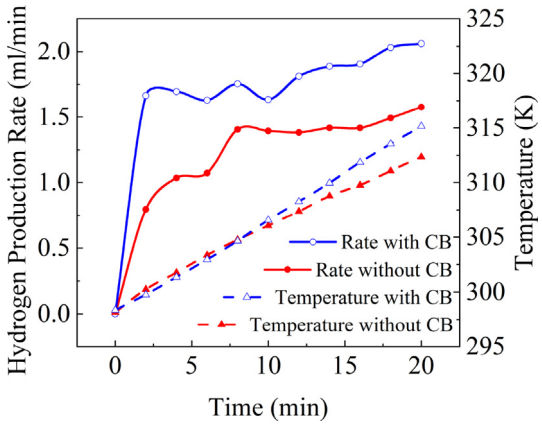

Fig. 12 – Comparison of production rate and temperature for electrolytes with and without CB.

also observed by other researchers. Ulset et al. [51] demonstrated that superheat of CB nanofluid steam was dependent on the CB concentration and reached a maximum value at 1 wt %. However, the maximum value occurred at 0.1 wt % and 0.001 wt % in our study. Because Ulset et al. heated the nanofluid until boiling, and the fluid did not reach the maximum temperature in their experiments, the temperature increasing rate may vary during the whole process that caused different results.

Comparison of CB effects

To have a more intuitive comparison of the effects of CB on a salt electrolyte, Fig. 12 shows the temperature and hydrogen production rate changes during the reaction for electrolytes with CB and without CB. The concentration of SS was 10 wt % for both electrolytes, and the concentration of CB was 0.1 wt %. During the first 8 min, there was no evident difference between the temperatures of the two electrolytes. When the reaction started, only CB on the surface of the electrolyte absorbed the heat, and CB in the inner part was unlikely to be radiated as the CB on the surface formed a "shield" to block the light. As a result, it was mainly thermal conduction in the electrolyte that induced the temperature to increase slowly. However, for electrolytes without CB, light could penetrate the solution due to its transparency, which means the temperature could increase fast. Therefore, the temperatures had the same increasing rate. However, during this period of time, the hydrogen production rates revealed high discrepancies. It is easier for a CB-based electrolyte to start the electrolysis at a higher reaction rate (1.66 ml/min) and maintain a slow growth rate due to the increased electrical conductivity of the electrolyte caused by the presence of CB. On the contrary, the hydrogen production rate for the SS solution starts at 0.79 ml/min, which is about half of the initial rate for a CB-based electrolyte, and then it increases fast. Compared with thermal properties, the electrical properties of CB have a greater impact on the process.

After 8 min, from Fig. 12, the impacts of thermal properties dominated the electrical properties. The temperature increases fast for CB-based electrolytes, and the hydrogen production rate also shows a visible rising trend. Similarly, the rate of hydrogen production and temperature for electrolytes without CB have an increasing trend, but they are significantly lower than electrolytes with CB. Heat conduction was strong during this time in the inner part of the electrolyte with CB, so the growth of temperature was faster. Afterwards, as mentioned before, the higher the temperature, the faster the tares. During the 20 min, the hydrogen production rates were 2.06 ml/min and 1.58 ml/min for electrolytes with CB and without CB, and the temperatures are 315.15 K and 312.35 K, respectively. Using CB makes the hydrogen production rate increase by 30.37%.

Electrolysis efficiency

In the previous sections, we found that CB does have positive effects on electrolysis. In this section, we evaluate the performance by estimating the efficiency of the process. For now, the objective of almost all the research for electrolysis is to increase electrolysis efficiency. Higher efficiency means less loss, and it can save energy.

There are numerous ways to evaluate the efficiency of an electrolyser. These include cell efficiency, energy efficiency, current efficiency, and thermal efficiency. Chakik et al. [52] summarized a model to calculate the electrolysis efficiency of water electrolysis:

$$\eta = \frac{V_{H_2}}{\frac{I \cdot V_m \cdot t}{2F}} \tag{10}$$

where η is the electrolysis efficiency, V_{H_2} is the volume of produced hydrogen, I is current, V_m is the molar volume (24.47 L/mol in 25 °C), t is reaction time and F is the Faraday constant (96 485 s A/mol).

In our study, the electrolysis efficiency can be calculated by:

$$\eta = \frac{E_{H_2}}{W_E} \tag{11}$$

$$E_{H_2} = n \cdot HHV \tag{12}$$

$$W_E = U \cdot I \cdot t, \tag{13}$$

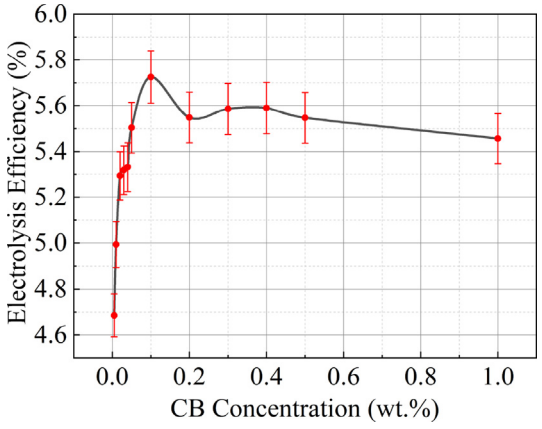

Fig. 13 – Electrolysis efficiency vs. CB concentration.

where E_{H_2} is the energy produced by electrolysis, i.e., energy stored in hydrogen, W_E is the energy consumed by electrolysis, i.e., electrical energy, n is the amount of substance, HHV is the higher heating value (=286 kJ/mol for hydrogen) and U is the voltage.

Fig. 13 shows the electrolysis efficiency for different CB concentrations. Similar to Fig. 9, one can clearly observe a rapid increase of efficiency with respect to concentration in cases when the concentration was low. For higher values of concentration, the efficiency decreases but with a lower rate. The maximum efficiency is 5.72% for the concentration 0.1 wt %, whereas the minimum efficiency is 4.69% for 0.005 wt%. This indicates that the efficiency increased by about 21.96%. These efficiencies are much lower than the industrial electrolysers as only simple electrodes and electrolytes were used, but the results are still meaningful. The reason is that the higher temperature induced a higher current and increased the consumption of electrical power. At first, temperature raises the ionic conductivity and enhances the current flow into the system. Therefore, the overall efficiency of the system in this work tends to increase with temperature. When increasing the concentration of CB, the temperature and the current density increase fast. As expressed by Ohm's law, the resistance in the system becomes more prominent when the current density increases. The efficiency of an electrolyser diminishes with increased temperature because at elevated temperatures the current density intensifies, resulting in higher activation and ohmic overpotentials. Another potential reason for the decrease is the coverage of the electrode surface by the NPs. The electrical double layer could catch the electrons that have a negative influence on the water electrolysis efficiency.

Concluding remarks

This study focused on the results of electrolyzing a carbon balance nanofluid-based electrolyte and analysed the effect of CB NF on the electrolysis. The results of the first part reveal that CB and light can increase the hydrogen production rate. The former increased the electrical conductivity of the electrolyte, and the latter increased the temperature of the electrolyte. The results of the second parts show that different CB concentrations have a different effect on the hydrogen production rate. The maximum hydrogen production rate occurred at the concentration of 0.1 wt %. When a screen was used to block the light, the maximum rate occurred at a concentration of 0.05 wt %. However, increasing the CB concentration leads to an increase in the hydrogen production rate up to the maximum value and then decreases for both situations. The results of the third part indicate that there may be a positive effect and negative effect of nanoparticles on the electrolysis as the average hydrogen production rates for every 2 min did not always increase or decrease. Thus, the whole electrolysis process can be treated as a "dynamic balance".

For a future work, other types of fluids can be tested. An example is the use of different nanofluids, not necessarily CB. Also, biodegradable fluids that have recently gained popularity [36] should also be considered.

Declaration of competing interest

The authors declare that they have no known competing financial interests or personal relationships that could have appeared to influence the work reported in this paper.

Acknowledgments

Shihao Wei gratefully acknowledges financial support from China Scholarship Council. Boris Balakin thanks Russian Foundation for Basic Research (Project 20–58-53022).

REFERENCES

[1] Guido Collodi, Wheeler Foster. Hydrogen production via steam reforming with CO2 capture. Chem Eng Trans 2010;19:37–42.
[2] Lewis Larry N. Chemical catalysis by colloids and clusters. Chem Rev 1993;93(8):2693–730.
[3] Godula-Jopek Agata. "Hydrogen Production: by electrolysis". en. 2015. p. 425. ZSCC: 0000074.
[4] Gandia Luis M, Arzamedi Gurutze, Diéguez Pedro M. Renewable hydrogen technologies: production, purification, storage, applications and safety. Newnes; 2013.
[5] Xu S, Zhao H, Li T, Liang J, Lu S, Chen G, Gao S, Asiri AM, Wu Q, Sun X. Iron-based phosphides as electrocatalysts for the hydrogen evolution reaction: recent advances and future prospects. J Mater Chem 2020;8(38):19729–45.
[6] Liu T, Liu D, Qu F, Wang D, Zhang L, Ge R, Hao S, Ma Y, Du G, Asiri AM, Chen L. Enhanced electrocatalysis for energy-efficient hydrogen production over CoP catalyst with nonelectroactive Zn as a promoter. Adv Energy Mater 2017;7(15):1700020.
[7] Zhang Y, Liu Y, Ma M, Ren X, Liu Z, Du G, Asiri AM, Sun X. A Mn-doped Ni_2 P nanosheet array: an efficient and durable hydrogen evolution reaction electrocatalyst in alkaline media. Chem Commun 2017;53(80):11048–51.
[8] Li X, Zhang R, Luo Y, Liu Q, Lu S, Chen G, Gao S, Chen S, Sun X. A cobalt–phosphorus nanoparticle decorated N-doped carbon nanosheet array for efficient and durable hydrogen evolution at alkaline pH. Sustain Energy Fuels 2020;4(8):3884–7.
[9] Gholamrezaei S, Ghiyasiyan-Arani M, Salavati-Niasari M, Moayedi H. Multidisciplinary methods (co-precipitation, ultrasonic, microwave, reflux and hydrothermal) for synthesis and characterization of $CaMn_3O_6$ nanostructures and its photocatalytic water splitting performance. Int J Hydrogen Energy 2019;44(48):26373–86.
[10] Ghanbari D, Salavati-Niasari M, Sabet M. Preparation of flower-like magnesium hydroxide nanostructure and its influence on the thermal stability of poly vinyl acetate and poly vinyl alcohol. Compos B Eng 2013;45(1):550–5.
[11] Salavati-Niasari M, Sobhani A, Davar F. Synthesis of star-shaped PbS nanocrystals using single-source precursor. J Alloys Compd 2010;507(1):77–83.
[12] Salavati-Niasari M, Davar F, Loghman-Estarki MR. Controllable synthesis of thioglycolic acid capped ZnS (Pn) 0.5 nanotubes via simple aqueous solution route at low temperatures and conversion to wurtzite ZnS nanorods via thermal decompose of precursor. J Alloys Compd 2010;494(1–2):199–204.

[13] Zinatloo-Ajabshir S, Morassaei MS, Salavati-Niasari M. Eco-friendly synthesis of $Nd_2Sn_2O_7$–based nanostructure materials using grape juice as green fuel as photocatalyst for the degradation of erythrosine. Compos B Eng 2019;167:643–53.
[14] Salavati-Niasari M. Zeolite-encapsulation copper (II) complexes with 14-membered hexaaza macrocycles: synthesis, characterization and catalytic activity. J Mol Catal Chem 2004;217(1–2):87–92.
[15] Salavati-Niasari M. Nanoscale microreactor-encapsulation 14-membered nickel (II) hexamethyl tetraaza: synthesis, characterization and catalytic activity. J Mol Catal Chem 2005;229(1–2):159–64.
[16] Razavi FS, Sobhani A, Amiri O, Ghiyasiyan-Arani M, Salavati-Niasari M. Green sol-gel auto-combustion synthesis, characterization and investigation of the electrochemical hydrogen storage properties of barium cobalt oxide nanocomposites with maltose. Int J Hydrogen Energy 2020 Jul 10;45(35):17662–70.
[17] Li Yanjiao, Zhou Jing'en, Tung Simon, Schneider Eric, Xi Shengqi. "A Review on Development of Nanofluid Preparation and Characterization". en. In: Powder Technology 196.2; Dec 2009. p. 89–101. ZSCC: NoCitationData [s1].
[18] Goudarzi K, Nejati F, Shojaeizadeh E, Asadi Yousef-abad SK. Experimental study on the effect of pH variation of nanofluids on the thermal efficiency of a solar collector with helical tube. Exp Therm Fluid Sci 2015;vol. 60:20–7.
[19] Maxwell JC. A treatise on electricity and magnetism, vol. 1. Clarendon Press; 1881.
[20] Choi Stephen US, Eastman Jeffrey A. Enhancing thermal conductivity of fluids with nanoparticles. Tech. rep. Argonne National Lab; 1995. IL (United States).
[21] Fendler Janos H. Colloid chemical approach to nanotechnology. Kor J Chem Eng 2001;18(1):1–13.
[22] Otanicar Todd P, Phelan Patrick E, Golden Jay S. Optical properties of liquids for direct absorption solar thermal energy systems. Sol Energy 2009;83(7):969–77.
[23] Otanicar Todd P, Phelan Patrick E, Ravi S Prasher, Gary Rosengarten, Taylor Robert A. Nanofluid-based direct absorption solar collector. J Renew Sustain Energy 2010;2(3). 033102.
[24] Prastiwi Yohanna. Unit operations of chemical engineering. 5th ed. Mc Cabe And Smith; 2008. English.
[25] Sani E, Mercatelli L, Barison S, Pagura C, Agresti F, Colla L, Sansoni P. Potential of carbon nanohorn-based suspensions for solar thermal collectors. Sol Energy Mater Sol Cell 2011;95(11):2994–3000.
[26] Han Dongxiao, Meng Zhaoguo, Wu Daxiong, Zhang Canying, Zhu Haitao. "Thermal Properties of Carbon Black Aqueous Nanofluids for Solar Absorption". en. Nanoscale Res Lett 2011;6(1):457. https://doi.org/10.1186/1556-276X-6-457. 1556-276X.
[27] Ganley Jason C. High temperature and pressure alkaline electrolysis. Int J Hydrogen Energy 2009;34(9):3604–11.
[28] Christopher MA. Brett and Ana Maria Oliveira Brett. Electrochemistry: principles, Methods, and Applications. en. Oxford Science Publications. Oxford; New York: Oxford University Press; 1993.
[29] Lobato J, Oviedo J, Cañizares P, Rodrigo MA, Millán M. Impact of carbonaceous particles concentration in a nanofluidic electrolyte for vanadium redox flow batteries. Carbon 2020;156:287–98.
[30] Bose P, Deb D, Bhattacharya S. Ionic liquid based nanofluid electrolytes with higher lithium salt concentration for high-efficiency, safer, lithium metal batteries. J Power Sources 2018;406:176–84.
[31] Yen PH, Wang JC. Power generation and electric charge density with temperature effect of alumina nanofluids using dimensional analysis. Energy Convers Manag 2019;186:546–55.
[32] Amin Asadi, Pourfattah Farzad, Miklós Szilágyi Imre, Afrand Masoud, Żyła Gaweł, Ahn Ho Seon, Wongwises Somchai, Nguyen Hoang Minh, Ahmad Arabkoohsar, Mahian Omid. "Effect of Sonication Characteristics on Stability, Thermophysical Properties, and Heat Transfer of Nanofluids: a Comprehensive Review". en. In: Ultrasonics sonochemistry 58; Nov 2019. p. 104701. ZSCC: NoCitationData[s1].
[33] Zhang C, Weldetsadik NT, Hayat Z, Fu T, Zhu C, Jiang S, Ma Y. The effect of liquid viscosity on bubble formation dynamics in a flow-focusing device. Int J Multiphas Flow 2019;117:206–11.
[34] Hwang Y, Lee JK, Lee JK, Jeong YM, Cheong SI, Ahn YC, Kim SH. Production and dispersion stability of nanoparticles in nanofluids. Powder Technol 2008;186(2):145–53.
[35] Ulset ET, Kosinski P, Balakin BV. Solar steam in an aqueous carbon black nanofluid. Appl Therm Eng 2018;137:62–5.
[36] Kosinska A, Balakin BV, Kosinski P. Use of biodegradable colloids and carbon black nanofluids for solar energy applications. AIP Adv 2021;11:055214.
[37] Romanelli MF, Moraes MCF, Villavicencio ALCH, Borrely SI. Evaluation of toxicity reduction of sodium dodecyl sulfate submitted to electron beam radiation. Radiat Phys Chem 2004;71(1–2):411–3.
[38] Lechuga M, Fernandez-Serrano M, Ríos F, Fernández-Arteaga A, Jiménez-Robles R. Environmental impact assessment of nanofluids containing mixtures of surfactants and silica nanoparticles. 2021.
[39] Godula-Jopek A. Hydrogen production: by electrolysis. John Wiley & Sons; 2015.
[40] Khani M, Habibzadeh S, Moraveji MK, Ebrahim HA, Alizadeh J. Novel α-alumina@ CuO-Fe_2O_3nanofluid for potential application in PEM fuel cell cooling systems: towards neutralizing the increase of electrical conductivity. Thermochim Acta 2021;695:178818.
[41] Shoghl SN, Jamali J, Moraveji MK. Electrical conductivity, viscosity, and density of different nanofluids: an experimental study. Exp Therm Fluid Sci 2016;74:339–46.
[42] Mashali F, Languri E, Mirshekari G, Davidson J, Kerns D. Nanodiamond nanofluid microstructural and thermo-electrical characterization. Int Commun Heat Mass Tran 2019;101:82–8.
[43] Ijam A, Saidur R, Ganesan P, Golsheikh AM. Stability, thermo-physical properties, and electrical conductivity of graphene oxide-deionized water/ethylene glycol based nanofluid. Int J Heat Mass Tran 2015;87:92–103.
[44] Maxwell JC. A treatise on electricity and magnetism, vol. 1. Oxford: Clarendon Press; 1873.
[45] Shen LP, Wang H, Dong M, Ma ZC, Wang HB. Solvothermal synthesis and electrical conductivity model for the zinc oxide-insulated oil nanofluid. Phys Lett 2012;376(10–11):1053–7.
[46] Lavasani AM, Vakili M. Experimental study of photothermal specifications and stability of graphene oxide nanoplatelets nanofluid as working fluid for low-temperature Direct Absorption Solar Collectors (DASCs). Sol Energy Mater Sol Cell 2017;164:32–9.
[47] Heyhat MM, Irannezhad A. Experimental investigation on the competition between enhancement of electrical and thermal conductivities in water-based nanofluids. J Mol Liq 2018;268:169–75.
[48] Mashali F, Languri E, Mirshekari G, Davidson J, Kerns D. Nanodiamond nanofluid microstructural and thermo-electrical characterization. Int Commun Heat Mass Tran 2019;101:82–8.

[49] Zawrah MF, Khattab RM, Girgis LG, El Daidamony H, Aziz REA. Stability and electrical conductivity of water-base Al2O3 nanofluids for different applications. HBRC journal 2016;12(3):227–34.
[50] Choi D, Lee KY. Experimental study on water electrolysis using cellulose nanofluid. Fluid 2020;5(4):166.
[51] Ulset ET, Kosinski P, Zabednova Y, Zhdaneev OV, Struchalin PG, Balakin BV. Photothermal boiling in aqueous nanofluids. Nano Energy 2018;50:339–46.
[52] Chakik FE, Kaddami M, Mikou M. Effect of operating parameters on hydrogen production by electrolysis of water. Int J Hydrogen Energy 2017;42(40):25550–7.